BONE MARROW DOSE IN FAST NEUTRON IRRADIATION CALCULATED FROM GEOMETRICAL BONE STRUCTURES (PART 1)

By

Osamu Yamamoto

Department of Radiation Biology (Prof. Dr. H. Yoshinaga),
Research Institute for Nuclear Medicine and Biology
Hiroshima University,
Hiroshima, Japan

幾何学的骨構造から計算される速中性子骨髄線量（その 1）

広島大学原爆放射能医学研究所 障害基礎部門
（主任 吉永春馬教授）
山 本 修

（昭和38年2月15日受付）

Spiers 理論をもとにして，骨髄エネルギー吸収の計算を14.1MeV 速中性子照射の場合についておこなつた．この計算ではX線，γ線の場合とは異つて，骨髄平面中の1点におけるエネルギー吸収は，中性子の入射方向に関してその点より線源側の骨と軟組織のみに影響されることを考慮した．これは陽子散乱が中性子の入射方向にたいして，中性子と水素核との衝突点より前方に生ずるからである．

計算の結果，骨髄中のエネルギー吸収は中性子線源側の骨と骨髄との内接面に近ずくにしたがつて減少する．これらのエネルギー吸収曲線はX線のそれとは逆の形をとり，骨が厚いほどエネルギー吸収の減少は著るしい．しかしながら，なお幾つかの補正の問題が残されている．

Introduction

In a previous paper[1] it was mentioned that the bone marrow had a elemental composition almost identical to other soft tissues, and therefore, it was concluded that the absorption dose of bons marrow would be the same as those of other soft tissues when estimated only from the elemental composition and not other factors.

However, the marrow is included in or surrounded by bone, which makes it different from the marrow in elemental composition. Discussion will be made in this paper whether such difference in elemental composition causes a difference in energy absorptions between X-ray or gamma-ray and fast neutron irradiations and whether such difference is associated with difference in injury mechanism.

A theoretical consideration of energy absorption by tissue was established by Spiers[2)3)]

in accordance with Gray's cavity theory. Thereafter, Woodard et al[4)5)]. studied the histochemical aspects of alkaline glycerophosphatase in bone marrow and developed the energy absorption concept which is based upon the ion pair in tissue in microscopical scale. Epp et al[6)]. and Sinclair[7)] applied this theory to various X-rays and gamma-rays of radium and cobalt-60 as a factor which affects LD_{50} or is related to its RBE. Recently Carlton and Cormack[8)] discussed the method of calculating the distribution of energy dissipated by electron near an interface and across a parallel slab or cylindrical cavity. The problem of alpha radiation dose was also presented by Kononenko[9)] and, Carlton and Cormack[10)]. This author utilizing the foregoing theoretical consideration wishes to discuss the energy absorption of marrow given by proton produced secondarily by 14.1 MeV fast neutron.

Table 1. Composition of metaphysical bone
(specific gravity=1.40)[6)]

Element	Atomic nubmer, Z	Fractional atomic content	Fractional electron content, a	Gm / 100gm	Electrons / gm	Electrons / cm^3
Ca	20	0.0368	0.153	16.10	0.484×10^{23}	0.678×10^{23}
S	16	0.0013	0.004	0.44	0.013×10^{23}	0.018×10^{23}
P	15	0.0209	0.065	7.06	0.206×10^{23}	0.288×10^{23}
O	8	0.3133	0.519	54.66	1.646×10^{23}	2.307×10^{23}
N	7	0.0247	0.036	3.77	0.113×10^{23}	0.158×10^{23}
C	6	0.0944	0.117	12.37	0.372×10^{23}	0.520×10^{23}
H	1	0.5086	0.106	5.59	0.334×10^{23}	0.467×10^{23}
Totals		1.0000	1.000	99.99	3.17×10^{23}	4.44×10^{23}

Effective $\overline{Z}=11.9$

Table 2. Composition of metaphysical soft tissue
(specific gravity=1.07*)

Element	Atomic number, Z	Fractional atomic content	Fractional electron content, a	Gm[1)2)] / 100gm	Electrons / gm	Electrons / cm^3
Ca	20	—	—	0.01	—	—
K	19	0.0006	0.003	0.35	0.010×10^{23}	0.011×10^{23}
Cl	17	0.0002	0.001	0.1	0.003×10^{23}	0.003×10^{23}
S	16	0.0004	0.002	0.2	0.006×10^{23}	0.006×10^{23}
P	15	0.0004	0.002	0.2	0.006×10^{23}	0.006×10^{23}
Mg	12	0.0001	—	0.04	0.001×10^{23}	0.001×10^{23}
Na	11	0.0003	0.001	0.1	0.003×10^{23}	0.003×10^{23}
O	8	0.2888	0.665	73	2.198×10^{23}	2.352×10^{23}
N	7	0.0181	0.036	4	0.120×10^{23}	0.128×10^{23}
C	6	0.0632	0.109	12	0.361×10^{23}	0.386×10^{23}
H	1	0.6279	0.181	10	0.598×10^{23}	0.640×10^{23}
Totals		1.0000	1.000	100	3.31×10^{23}	3.54×10^{23}

Effective $\overline{Z}=8.2$

* This value was experimentally obtained from the organs of mice.

The Composition of Bone and Bone Marrow

To estimate the energy absorption of the bone marrow, the composition of bone and bone marrow should be determined. The compositions of bone and bone marrow as a soft tissue are as shown in Table 1 and 2.

Calculation Method of Energy Absorption

Spiers has developed a method for calculating energy absorption in the soft tissue medium adjacent to the semi-infinite layer of bone. This method was expanded by Epp et al. and Sinclair for the case where the bone layer is thinner than the electron ranges. In the present paper, the method is used to compare the average energy absorptions in tissue layers of variable thickness between two layers of bone for 14.1 MeV fast neutron. Neutron energy is transferred to proton which is produced secondarily, and then the proton energy is absorbed by the tissue. For the calculation of energy absorption by tissue, back scattering need not be considered in the case of fast neutron irradiation. There is, therefore, some difference in the calculation from the case of X-rays and gamma-rays.

1. *The case of semi-infinite bone and soft tissue plane interface.*

A. When the neutron incidence direction is toward the tissue layer from the bone layer, the energy absorption contributed at point P in the soft tissue at distance d from the plane interface of a semi-infinite layer of bone and a finite layer of tissue (Fig. 1-1) by protons produced secondarily in the bone can be derived by the formula

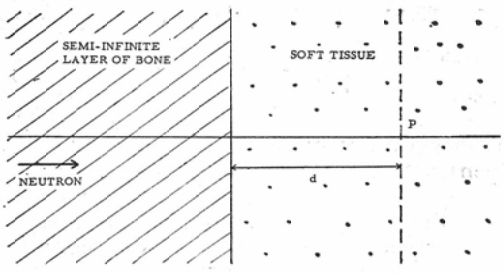

Fig. 1-1. Semi-infinite bone, soft tissue plane interface.

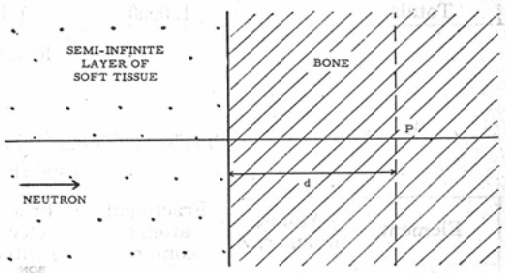

Fig. 1-2. Semi-infinite soft tissue, bone plane interface.

$$TD_B = \sum \frac{N_B E_B}{\rho_T} f\left(\frac{d}{R_T}\right) \text{ ergs/cm}^3\text{/neutron} \qquad (1)$$

where N_B= number of protons of initial energy E_B (ergs) arising in bone per cubic centimeter per unit flux of neutron, ρ_T=ratio of stopping power of bone to that of soft tissue, R_T=range in soft tissue of a proton of energy E_B, and

$$f\left(\frac{d}{R_T}\right) = 1 + \frac{d}{R_T}\left[\ln\left(\frac{d}{R_T}\right) - 1\right].$$

The sum is the pronton energies produced secondarily in the bone. The energy absorption at the same point contributed by protons produced secondarily in the finite layer of tissue d micron in thickness is given by

$$TD_T = \sum N_T E_T \left[1 - f\left(\frac{d}{R_T}\right) \right] \text{ ergs/cm}^3\text{/neutron} \qquad (2)$$

where N_T = number of protons of initial energy E_T arising secondarily in soft tissue per cubic centimeter per unit flux of neutron.

B. On the contrary, when the neutron incidence direction is toward the bone layer from soft tissue layer, the energy absorption in bone interfacing a semi-infinite layer of soft tissue is also treated on the same way as above. Then at point P (Fig. 1-2) the energy absorption is given by

$$BD_T = \sum \frac{N_T E_T}{\rho_B} f\left(\frac{d}{R_B}\right) \text{ ergs/cm}^3\text{/neutron} \qquad (3)$$

and

$$BD_B = \sum N_B E_B \left[1 - f\left(\frac{d}{R_B}\right) \right] \text{ ergs/cm}^3\text{/neutron} \qquad (4)$$

where ρ_B = ratio of stopping power of soft tissue to that of bone, R_B=range in the bone of a proton of energy E_T, and

$$f\left(\frac{d}{R_B}\right) = 1 + \frac{d}{R_B}\left[\ln\left(\frac{d}{R_B}\right) - 1 \right].$$

2. The case of a soft tissue layer between two semi-infinite layers of bone.

Generally, when material containing hydrogen nuclei is irradiated by neutrons, the proton scattering takes place in front of the neutron collision point from the incidence direction of neutrons, and the energies absorbed in the proton scattering directions[12]. Then only the effect on the bone and soft tissue of this side of the point p (Fig. 2) from the neutron incidence direction need to be considered. The calculation of this case, therefore, may be treated identical to Case 1.

3. The case of finite layer of bone adjacent to soft tissue.

The case of a finite layer of bone will be treated. Fig. 4 shows point P in soft tissue at distance d from plane bone layer of thickness D. On the other side of the bone layer is a semi-infinite layer of tissue, replacing the semi-infinite layer of bone in Fgi. 1. The

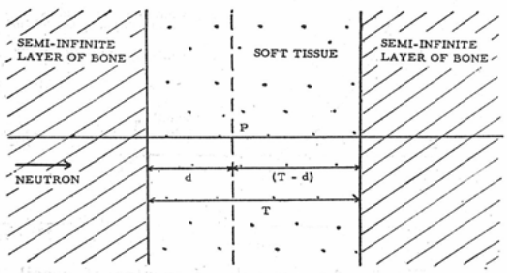

Fig. 2. Soft tissue layer between two semi-infinite thickness of bone.

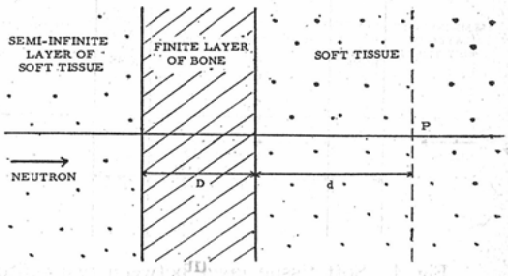

Fig. 3. Finite layer of bone adjacent to soft tissue.

As the contributions of bone layer and soft tissue layer respectively, Spiers has given the following equations for the absorption energy calculation with X-ray radiations:

$$D_B = \sum \frac{N_B E_B}{2\rho} f\left(\frac{d}{R_T}\right) \text{ ergs/cm}^3\text{/r}, \quad D_T = \sum \frac{N_T E_T}{2} \left[1 - f\left(\frac{d}{R_T}\right) \right] \text{ ergs/cm}^3\text{/r}.$$

contribution to the energy absorption at P by protons produced secondarily in the semi-infinite layer of tissus is derived by

$$TD_{T'}=\sum N_T\ E_T\ f\left(\frac{d+\rho_T D}{R_T}\right)\ \text{ergs/cm}^3\text{/neutron} \qquad (5)$$

where

$$f\left(\frac{d+\rho_T D}{R_T}\right)=1+\left(\frac{d+\rho_T D}{R_T}\right)\left[\ln\left(\frac{d+\rho_T D}{R_T}\right)-1\right]$$

This expression is identical to expression (1) except for the absence of the stopping power ratio ρ_T in the denominator of the first factor and the re-replacement of d by $(d+\rho_T D)$, where $\rho_T D$ represents the equivalent tissue thickness of the bone layer. The energy absorption at the same point contributed by protons produced secondarily in the finite layer of bone D microns in thickness is derived by

$$TD_{B'}=\sum\frac{N_B\ E_B}{\rho_T}\ f\left(\frac{d}{R_T}\right)-\sum\frac{N_B\ E_B}{\rho_T}\ f\left(\frac{d+\rho_T D}{R_T}\right)\ \text{ergs/cm}^3\text{/neutron} \qquad (6)$$

The first term in expression (6) represents the energy absorption at distance d from a semi-infinite layer of bone, and the second term represents a deduction of the contribution from a semi-infinite layer of bone at distance $(d+\rho_T D)$.

4. *The case of soft tissue layer between two finite thickness of bone.*

Unlike the cases of X-rays and gamma-rays, only the effect of the bone and the soft tissues of this side of point P (Fig. 4) from the neutron incidence direction need to be considered for the same reason as Case 2. Therefore, the absorption energy at point P is obtained in the same manner as Case 3.

Calculation of Energy Absorption for 14.1 MeV Fast Neutron

The initial energies and numbers of protons set in motion in soft tissue and bone by 14.1 MeV neutrons were obtained in the following manner. The recoil proton energy spectrum from a 14.1 MeV neutron source generator is shown in Fig. 5.

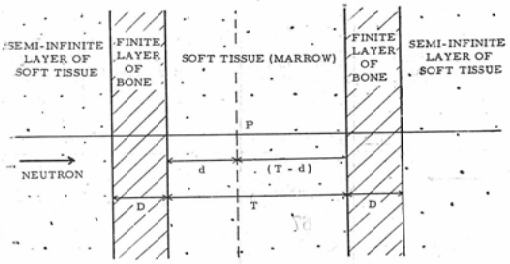

Fig. 4. Soft tissue layer between two finite thickness of bone.

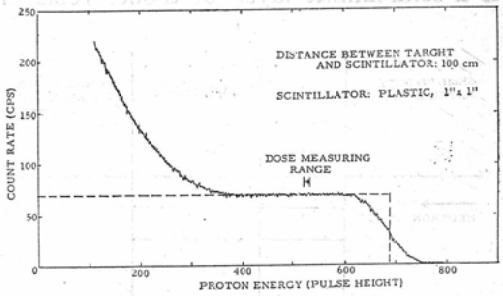

Fig. 5. An example of spectra of recoil proton produced in scintillator.

The rise in the curve in the low energy range is due to recoil C-nuclei, gamma-ray or noise of the counter itself. The broken line given as the theoretical recoil proton spectrum shows the real relative proton numbers. These are of the same height in the energy range of 0~14.12 MeV. In the calculation the energy range was divided into ten

and the average energy value in the divided range was used.

The number of protons N was derived from $n\rho$ (Table 3), the product obtained by multiplying the number of atom per cubic centimeter n by the cross section of each element, σ. Probabilities of collision between hydrogen atoms and neutrons in bone and soft tissue were estimated by the following:

$$P_B = \frac{(n_H\sigma_H)_B\left\{1-e^{-\Sigma(n_i\sigma_i)_B}\right\}}{(n_i\ \sigma_i)_B} = 0.0309$$

$$P_T = \frac{(n_H\sigma_H)_T\left\{1-e^{-\Sigma(n_i\sigma_i)_T}\right\}}{(n_i\ \sigma_i)_T} = 0.0419$$

where

$$\Sigma\ (n_i\sigma_i)_B=(n_{Ca}\sigma_{Ca})_B+(n_S\sigma_S)_B+(n_P\sigma_P)_B+(n_O\sigma_O)_B+(n_N\sigma_N)_B+(n_C\sigma_C)_B+(n_H\sigma_H)_B$$

and

$$\Sigma(n_i\sigma_i)_T=(n_K\sigma_K)_T+(n_{Cl}\sigma_{Cl})_T+(n_S\sigma_S)_T+(n_P\sigma_P)_T+(n_{Mg}\sigma_{Mg})_T+(n_{Na}\sigma_{Na})_T+(n_O\sigma_O)_T+(n_N\sigma_N)_T+(n_C\sigma_C)_T+(n_H\sigma_H)_T.$$

Table 3. The values of n, σ and $n\sigma$ for bone and soft tissue.

Bone			
Element	Atoms/cm³, n	Cross section, σ (barn)	$n\sigma$
Ca	0.0339×10^{23}	2.19[14)15)17)]	0.7424×10^{-2}
S	0.0012×10^{23}	1.92[16)18)]	0.0230×10^{-2}
P	0.0192×10^{23}	1.97[14)16)]	0.3782×10^{-2}
O	0.2881×10^{23}	1.590[13)]	4.5808×10^{-2}
N	0.0227×10^{23}	1.600[13)]	0.3632×10^{-2}
C	0.0868×10^{23}	1.350[13)]	1.1172×10^{-2}
H	0.4676×10^{23}	0.689[13)]	3.2218×10^{-2}
Soft tissue			
Element	Atoms/cm³, n	Cross section, σ (barn)	$n\sigma$
Ca	—	—	—
K	0.0006×10^{23}	2.24[14)]	0.0134×10^{-2}
Cl	0.0002×10^{23}	2.00[14)16)]	0.0040×10^{-2}
S	0.0004×10^{23}	1.92[14)18)]	0.0077×10^{-2}
P	0.0004×10^{23}	1.97[14)16)]	0.0079×10^{-2}
Mg	0.0001×10^{23}	1.75[16)20)]	0.0018×10^{-2}
Na	0.0002×10^{23}	1.71[18)19)]	0.0024×10^{-2}
O	0.2941×10^{23}	1.590[13)]	4.6762×10^{-2}
N	0.0184×10^{23}	1.600[13)]	0.2944×10^{-2}
C	0.0644×10^{23}	1.350[13)]	0.8694×10^{-2}
H	0.6397×10^{23}	0.689[13)]	4.4075×10^{-2}

In light of the probability of collision between one neutron and the hydrogen atoms in unit cubic centimeter and the division of the energy range into ten N_B ($0.0309\times1/10=3.09\times10^{-3}$) and N_T ($0.0419\times1/10=4.19\times10^{-3}$) were obtained respectively.

The radiation stopping power of materials can be expressed by

$$-\frac{dE}{dx}=\frac{4\pi e^4 z^2 n}{mv^2}B \quad [21]$$

where e = charge number of electrons, z =charge number of particles, n = number of atoms per cubic centimeter, m = mass of electron, v = particle velocity, $B = Z \ln 2mv^2/I$ (when the particle velocity is not as large as the expected the relative velocity effect), $I \doteqdot 11.5\ Z$, Z = effective atomic number.

The stopping powers of bone and soft tissue are obtained as follows.

$$S_B=\frac{4\pi e^4 z^2 n_B Z_B}{mv^2}\ln\frac{2mv^2}{11.5Z_B}, \quad \text{and} \quad S_T=\frac{4\pi e^4 z^2 n_T Z_T}{mv^2}\ln\frac{2mv^2}{11.5Z_T}.$$

Call $E = 1/2\ Mv^2$, where E = initial energy of particle and M = mass of particle. Then, $v^2 = 2E/M$. Thus,

$$\frac{S_B}{S_T}=\frac{n_B Z_B \ln\frac{4mE}{11.5\ Z_B M}}{n_T Z_T \ln\frac{4mE}{11.5\ Z_T M}}=\rho_T=\frac{1}{\rho_B}$$

ρ_T and ρ_B are shown in the last two columns of Table 4.

Table 4. Ranges of proton in bone and tissue, and ratio of stopping power between bone and tissue.

Proton energy (MeV)	R_{air} (cm)	R_B (μ)	R_T (μ)	ρ_B	ρ_T
0.706	1.33	13.8	11.1	0.7526	1.3288
2.118	7.55	80.4	64.5	0.7520	1.3297
3.530	18.50	192.1	154.0	0.7517	1.3303
4.942	33.00	342.6	274.8	0.7516	1.3305
6.354	51.50	534.7	428.8	0.7514	1.3308
7.766	73.50	763.1	612.0	0.7514	1.3309
9.178	98.70	1024.7	821.8	0.7512	1.3312
10.590	127.3	1321.6	1059.9	0.7511	1.3313
12.002	158.0	1640.4	1315.5	0.7511	1.3314
13.414	194.0	2041.1	1615.3	0.7510	1.3316

Although the research on the ranges of proton, deuteron and triton is not advanced as that of α-particle, it is known, however, with regard to the relation between proton and the range that the formula $R = (E/9.3)^{1.8}$ presented by Brobeck and Wilson can be applied to a considerable wide range from a few MeV to 200 MeV. In this paper the estimation of proton range in air is based on the energy curve prepared by Segré[22]. The proton range in other materials can be derived from the range in air by the following formula in all cases

$$R_A = R_{air} \times \frac{\text{Density of air}}{\text{Density of material A}} \times \frac{\text{Average mass number of material A}}{\text{Average mass number of air}} \times \sqrt{\frac{Z+10}{0.563\,Z}}$$

where R_A = range of particle in material A, R_{air} = range of particle in air, Z = effective atomic number.

Lastly, using the above calculated values, energy absorptions obtained by tne equations in the last chapter were totalled. The average energy absorptions in tissue layer of

variable thickness interfaced with bones of variable thickness were compared.

Discussion

When a semi-infinite layer of tissue interfaces a semi-infinite layer of bone and the neutron incidence direction is toward the bone layer from the tissue layer, the absorption energy in the bone layer decreases with distance from the interface and settles to a constant value at the place that corresponds to the maximum range of protons (Fig. 6-1). When neutron incidence direction is toward the tissue layer from the bone layer, the energy absorption in the tissue layer increases with distance from the interface and reaches to a constant value at the place that corresponds to the maximum range of protons (Fig. 6-2). This constant value corresponds to that given by Tochilin et al[23]. for the collision between hydrogens and neutrons.

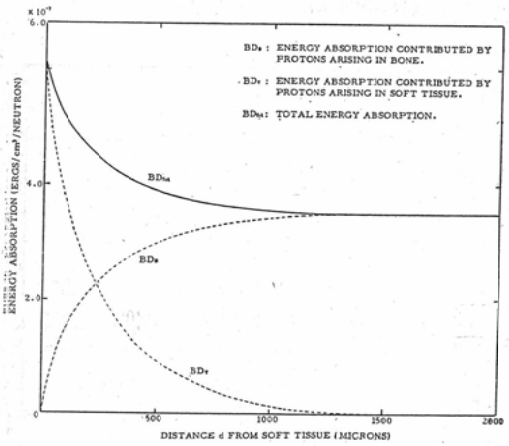

Fig. 6-1. Energy absorption curve in bone layer interfaced with semi-infinite soft tissue layer.

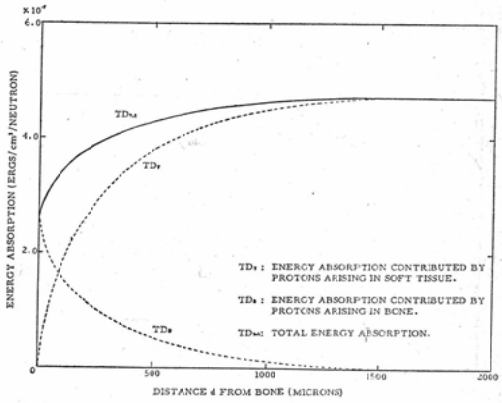

Fig. 6-2. Energy absorption curve in soft tissue layer interfaced with semi-infinite bone layer.

Next, the energy absorption of tissue layer sandwiched between two bone layers is considered. When the bone layer thickness is fixed, the energy absorption increases with distance toward the tissue layer below the maximum range of protons as above mentioned.

For the bone layer thicknesses of 50, 100, 200, 500 and 1000 microns, the energy absorption curves are shown in Fig. 7-1～5. With increase in bone thickness, the recoil proton energy of the bone is more effective for marrow energy absorption and at the same time the recoil proton energy of the outer tissue becomes less effective. The change in average energy absorptions is shown in Fig. 8. When the marrow layer thickness is fixed and the bone layer is variable, the decrease in energy absorption becomes more conspicuous with decrease in distance from the interface as seen in the figure. In Fig. 9 the changes in average energy absorptions where the bone layers are semi-infinite and 50 microns are compared for 250 kV X-ray, Co^{60} gamma-ray and 14.1 MeV neutron. The average energy absorption curves of the X-rays and the neutrons are in reverse relation

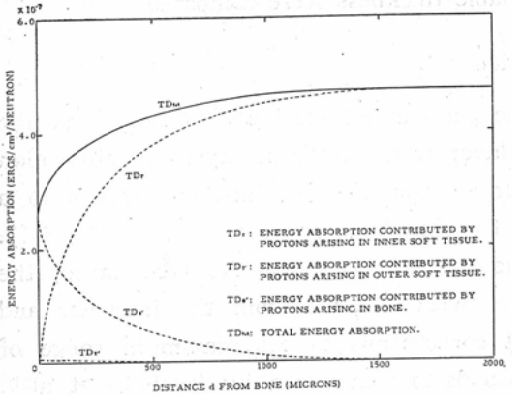

Fig. 7-1. Energy absorption curve in soft tissue layer interfaced with finite bone layer (D=1000μ).

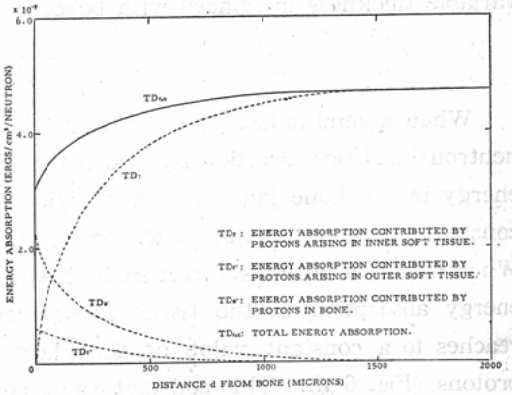

Fig. 7-2. Energy absorption curve in soft tissue layer interfaced with finite bone layer (D=500 μ).

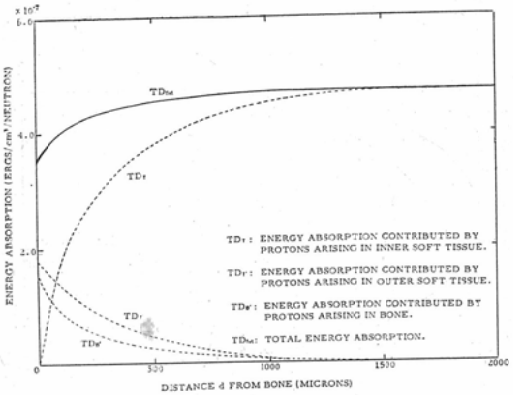

Fig. 7-3. Energy absorption curve in soft tissue layer interfaced with finite bone layer (D=200 μ).

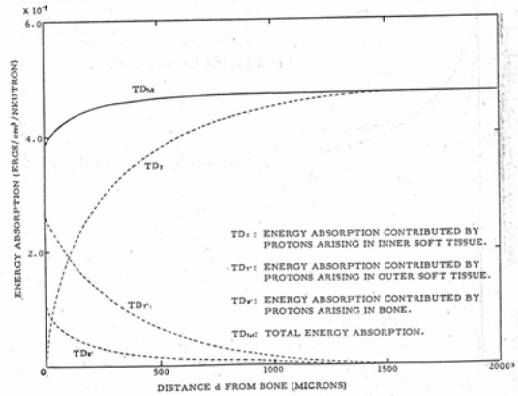

Fig. 7-4. Energy absorption curve in soft tissue layer interfaced with finite bone layer (D=100 μ).

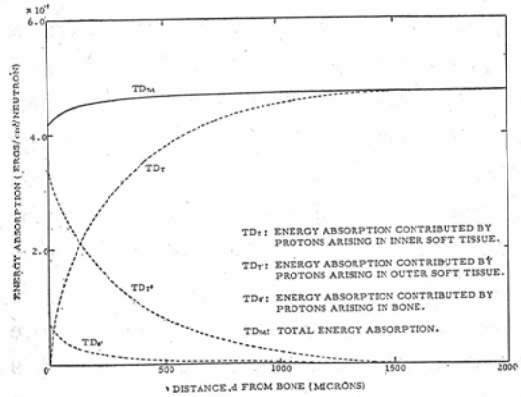

Fig. 7-5. Energy absorption curve in soft tissue layer interfaced with finite bone layer (D=50 μ).

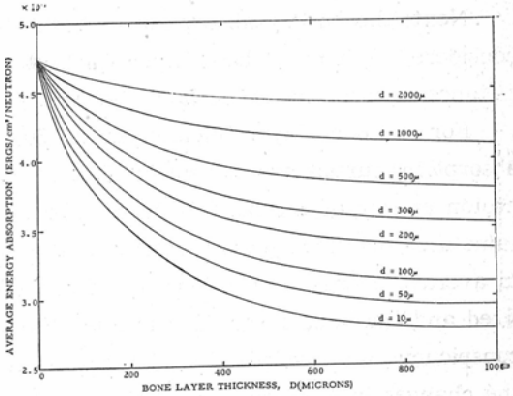

Fig. 8. The relation between bone layer thickness and average energy absorption.

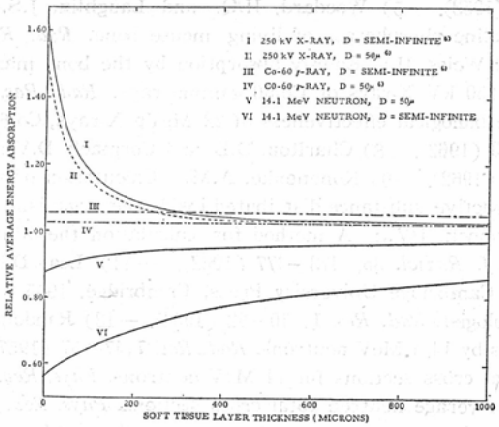

Fig. 9. Average energy absorption in soft tissue (marrow) between various thickness of bone.

with each other.

In this comparison, however, the effects of carbons, nitrogens and oxigens in soft tissue are not considered. Moreover, the distribution angle of protons produced secondarily with neutrons should also be taken into consideration. In next paper, corrections will be made for these points and a comparative study will be attempted for the total marrow doses of small animals by X-ray-, gamma-ray- and neutron-irradiations.

Summary

Based upon Spiers' theory, calculation of energy absorptions was done for 14.1 MeV fast neutrons. In this calculation, unlike X-ray and gamma-ray cases, the energy absorption at point P in a plane of bone marrow was calculated for only the effect on the bone and the soft tissues on this side of point P from the neutron incidience direction. This is because proton scattering takes place in front of the collision point with the neutron from the neutron incidence direction.

As the result of calculation, the energy absorption in bone marrow decreases with decrease in distance from the interface between the bone and the bone marrow in the side of neutron source. These energy absorption curves were opposite in shape to those of X-rays. The thicker the bone layer, the decrease in the energy absorption becomes more conspicuous. However, some correction must be done.

References

1) Yamamoto, O., Sawada, S. and Yoshinaga, H.: Fast neutron absorption dose estimated from the elemental constitution of bone marrow of small animals. *Nipp. Act. Radiol.* **23**, 141—145 (1963). — 2) Spiers, F.W.: The influence of energy absorption and electron range on dosage in irradiated bone. *Brit. J. Radiol.* **22**, 521— 533 (1949). — 3) Spiers, F.W.: Radiothrapeutic physics. II. Dosage in irradiated soft tissue and bone. *Brit. J. Radiol.* **24**, 365—368 (1951). — 4) Woodard, H.Q. and Spiers, F.W.: The effect of X-rays of different qualities on the alkaline phosphatase of living mouse bone.

Brit. J. Radiol. **26**, 38—46 (1953). —5) Woodard, H.Q. and Laughlin, J.S.: The effect of X-rays of different qualities on the alkaline phosphatase of living mouse bone. *Rad. Res.* **7**, 236—252 (1957). —6) Epp, E.R., Woodard, H.Q. and Weiss, H.: Energy absorption by the bone marrow of the mouse receiving whole-body irradiation with 250 kV X-rays or Co-60 gamma rays. *Rad. Res.* **11**, 184—197 (1959). —7) Sinclair, W.K.: The relative biological effectiveness of 22 MeVp X-rays, Co-60 gamma rays, and 200 kVcp X-rays. *Rad. Res.* **16**, 369—383 (1962). —8) Charlton, D.E. and Cormack, D.V.: Energy dissipation in finite cavities, *Rad. Res.* **17**, 34—49 (1962). —9) Kononenko, A.M.: Calculation of the intensity of the alpha-radiation dose arising a radioactive substance distributed inside the organism. *Biofizika* **2**, 98—117 (1957). —10) Charlton, D.E. and Cormack, DV..: A method for calculation the alpha-ray dosage to soft tissue-filled cavities in bone. *Brit. J. Radiol.* **35**, 473—477 (1962). —11) Lea, D.E.: Action of radiations on living cells (2nd ed.), p. 7, Cambridge University Press, Cambridge, 1955. —12) Moyer, B.J.: Neutron physics of concern to the biologist. *Rad. Res.* **1**, 10—22 (1954). —13) Randolph, M.L.: Energy deposition in tissue and similar materials by 14.1 MeV neutrons. *Rad. Res.* **7**, 47—57 (1957). —14) Coon, J.H., Graves, E.R. and Barshall, H.H.: Total cross sections for 14 MeV neutrons. *Phys. Rev.* **88**, 562—564 (1953). —15) Nereson, N. and Darden, S.: Average neutron total cross sections. *Phys. Rev.* **89**, 775—785 (1953). —16) Nereson, N. and Darden, S.: Average neutron total cross sections. *Phys. Rev.* **94**, 1678—1682 (1954). —17) Conner, J.P.: Total cross sections near 14.1 MeV. *Phys. Rev.* **109**, 1268—1272 (1958). —18) Hildebrand, R.H. and Leith, C.E.: Total cross sections of nuclei for 42 MeV neutrons. *Phys. Rev.* **80**, 842—845 (1950). —19) Wapstra, A.H.: Isotopic masses. *Physica* **21**, 367—409 (1955). —20) Bratenahl, A., Peterson, J.M. and Stoering, J.P.: Neutron total cross sections in the 7- to 14-MeV region. *Phys. Rev.* **110**, 927—936 (1958). —21) Bethe, H.A. and Ashkin, J.: see 22), p. 166. —22) Segré, E.: Experimental nuclear physics. Vol. 1, John Wiley & Sons,Inc., New York, 1953. —23) Tochilin, E., Ross, S.W., Shumway, B.W., Kohler, G.D. and Golden, R.: Cyclotron neutron and γ-ray dosimetry for animal irradiation studies. *Rad. Res.* **4**, 158—173 (1956).